AGU PUBLICATIONS

Geophysical Research Letters

Supporting Information for

Slip-pulse rupture behavior on a 2 meter granite fault

Gregory C. McLaskey

Cornell University, Ithaca, NY

Brian D. Kilgore

US Geological Survey, Menlo Park, CA

Nicholas M. Beeler

US Geological Survey, Menlo Park, CA

Contents of this file

Introduction

The seven supporting figures and two supporting tables provide additional information about the laser vibrometer results, the termination of slip pulses, 2D effects, the details of different recording instruments, and the kinematics of individual slip pulses.

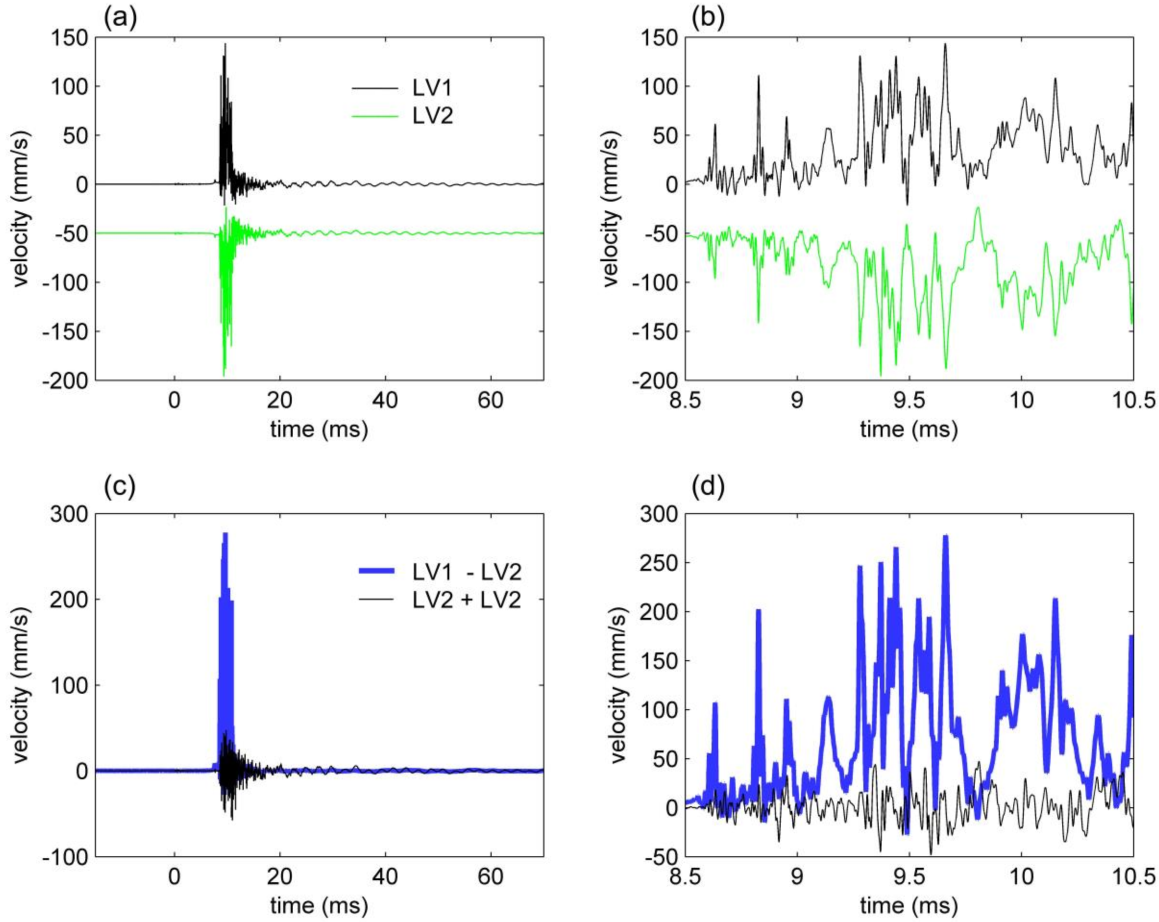

Figure S1. Details of laser-vibrometer-derived slip rate measurement for DSE13May2014. The two laser vibrometers (LV1 and LV2) were mounted on tripods that stood on the floor about 1 meter from the apparatus. The laser beams were aimed at reflective targets located on opposite sides of the fault as depicted in Figure 1a. The reflective targets were mounted to ~5 mm tall aluminum blocks that were glued directly to the top surface of the rock sample. **a**, The raw output from the two individual laser vibrometer readings (LV2 is offset -50 m/s for clarity). **b,** A zoom in on first strong motions. **c**, The heavy blue trace is LV1 – LV2 while the thin black trace is LV1 + LV2. **d**, A zoom in on the first strong motions. The large peaks in velocity produce an antisymmetric response on opposite sides of the fault, and we interpret LV1-LV2 (heavy blue trace) to be a measure of the fault slip rate, reported in Figure 2. On the other hand, later in the record (between 20 and 40 ms) LV1+LV2 (thin black trace) dominates the signal indicating that most of the ground velocity is due to coherent lower frequency vibrations of the sample rather than fault slip.

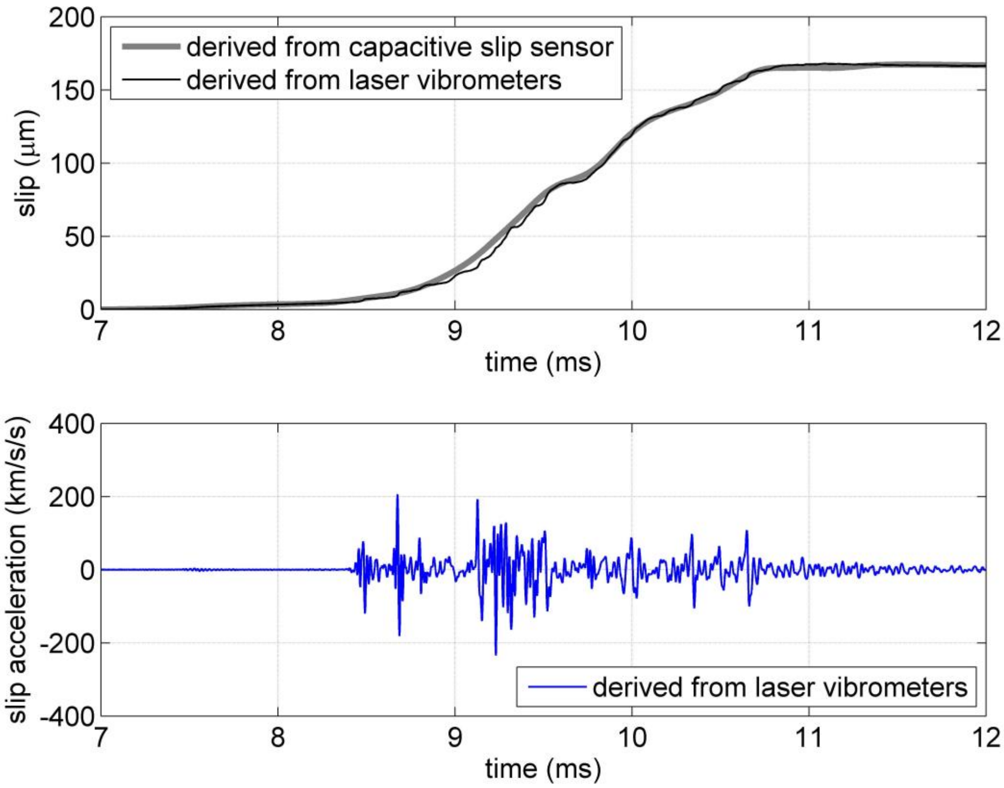

Figure S2. Upper plot, local fault slip from DSE13May2014 estimated by integrating the laser-vibrometer derived slip rate. This is compared to fault slip measured from the nearest capacitive slip sensor. Lower plot, local fault acceleration from the first derivative of laser-vibrometer derived slip rate for the same slip event.

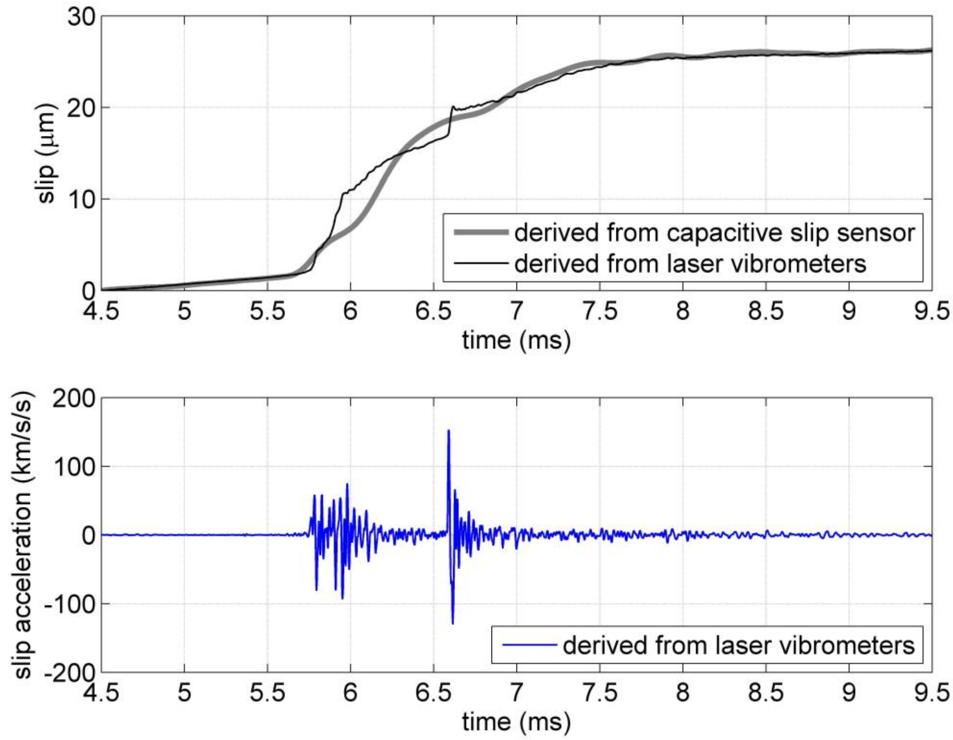

Figure S3. Same as Figure S2 but for DSE16May2014. Upper plot: local fault slip estimated by integrating the laser-vibrometer derived slip rate is compared to fault slip measured from the nearest capacitive slip sensor. Lower plot: local fault acceleration from the first derivative of laser-vibrometer derived slip rate.

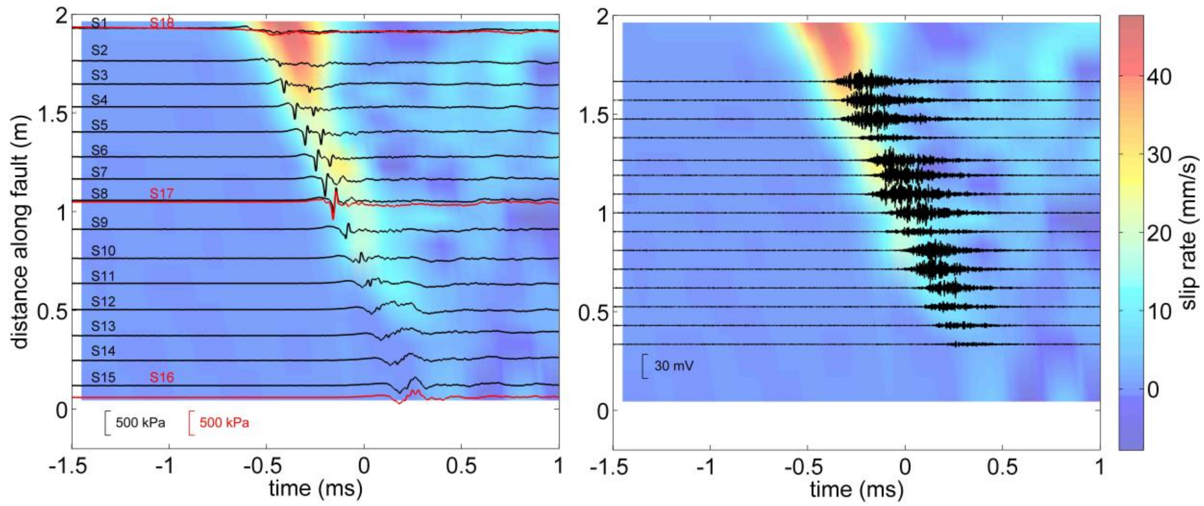

Figure S4. Same as Figure 3 a, b, except a different DSE (DSE18$_{Nov2012}$) which shows a slip pulse that terminates about two thirds of the way down the fault (at about 0.8 m, -0.25 ms). Before this DSE initiated, the fault had accumulated a large amount of aseismic slip on one end of the fault (close to S15) and the drop in shear stress associated with this aseismic slip appears to have been enough to cause the slip pulse to terminate.

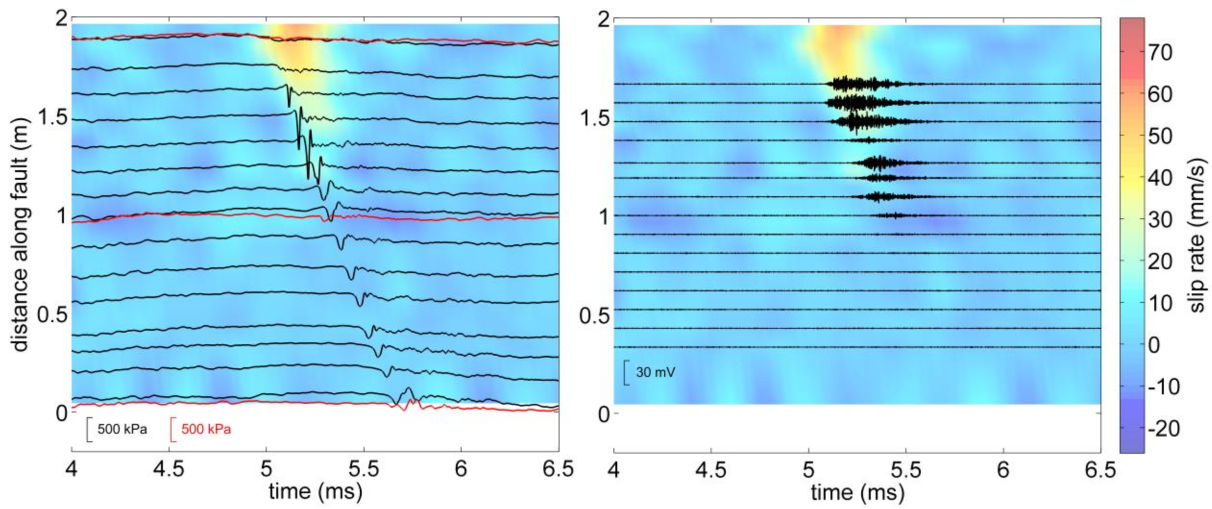

Figure S5. Same as Figure S4 except a different DSE (DSE17$_{Nov2012}$, a small slip event that occurs about 3 ms after the main dynamic rupture) which shows a slip pulse that terminates about one third of the way down the fault (at about 1.2 m, 5.25 ms).

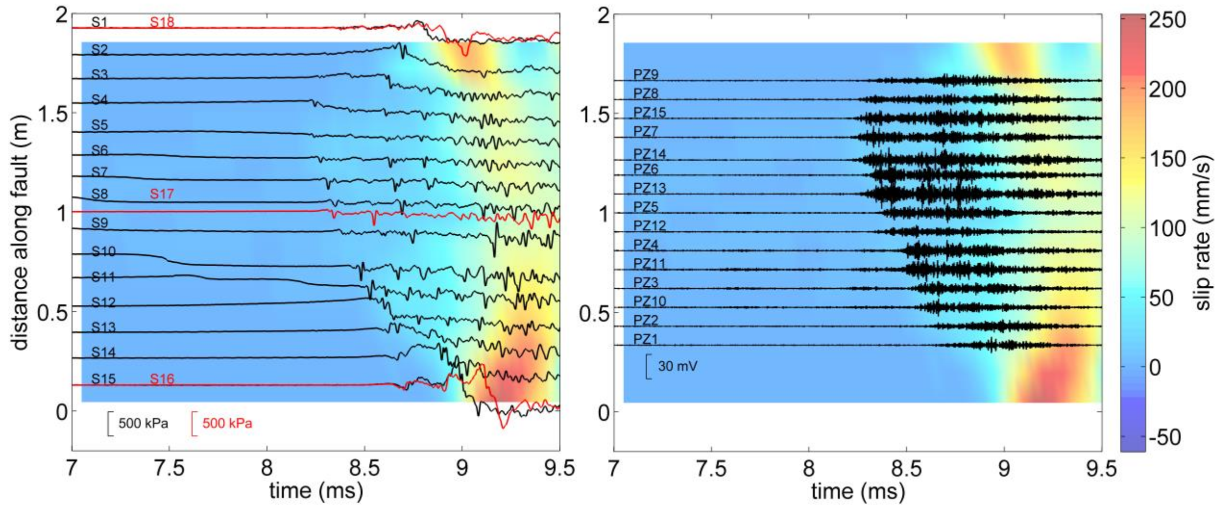

Figure S6, same as Figure 3 a, b, just zoomed in to show how the first slip pulse appears to terminate as it reaches the edge of the expanding nucleation zone at about 0.5 m, 8.6 ms.

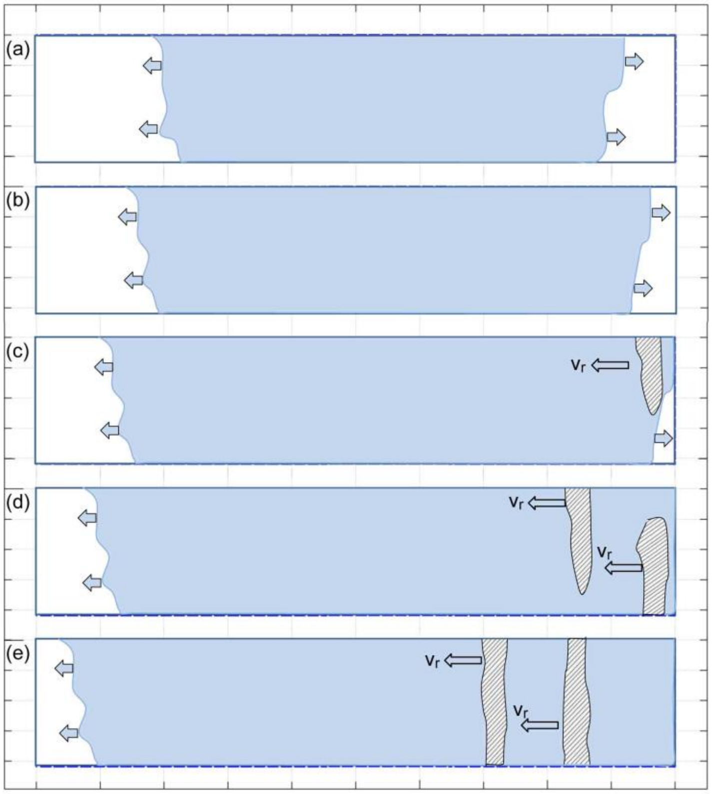

Figure S7. Cartoon showing how 2D effects may cause trains of slip pulses that are commonly observed in these experiments. The panels (**a-e**) are meant to depict successive snapshots of slip rate on the 2 m by 400 mm fault plane. (**a-b**) The light blue indicates the nucleation zone that is slowly slipping (0.01 to 1 mm/s). The nucleation zone expands at a rate of 10-1000 m/s until it reaches the end of the sample (**c**). At this point, the fault begins to slip rapidly, shear stress measured near the fault end drops, and a rapid fluctuation in shear stress, indicative of a slip pulse, propagates back across the sample at an apparent velocity v_r, which ranges from 80% - 100% the shear wave velocity in the granite. In many cases, sensors located on the top surface of the sample detect this fault slip and stress drop about 100-200 microseconds before the stress drop is detected by sensors on the bottom of the sample (compare the S15 and S16 in Figure 1b, 3a, and 3c). This indicates that the top part of the sample end slipped and began to generate a slip pulse before the bottom part of the sample end began to slip. Stress perturbations indicative of slip pulses typically occur simultaneously on strain gage pairs located on the top and bottom of the sample (compare red and black traces in Figure 1b, Figure 3a, and Figure 3c). This indicates that the slipping patch typically spans the full thickness of the sample. Sometimes there is a time delay (up to 100 microseconds) or amplitude discrepancy between the stress fluctuations observed by top and bottom gages. (For example, the second pulse detected by S17 in Figure 3a.) This indicates that pulse width or pulse slip velocity is sometimes nonuniform with depth.

Sensor type	Number of sensors	Locations	Quantity detected	Frequency Band	Sampling rate and recording mode
Piezoelectric	15	200 mm off the fault on both sides of fault and on top and bottom surfaces	vertical ground motion [b]	~100 Hz to > 1 MHz	5 MHz triggered
Capacitive Slip	16	straddling the top trace of the fault	local fault slip	~DC to 3 kHz	1 MHz triggered and 1 KHz continuous
Strain Gage Pairs	18	13 mm from the top trace of the fault, three gage pairs located on the bottom of the sample, 13 mm from the fault.	local shear strain	~DC to 500 kHz	1 MHz triggered and 1 KHz continuous
Laser Vibrometers	2 [a]	reflective targets located a few cm on either side of the top trace of the fault	velocity of the target relative to a (stationary) tripod.	~DC to 250 kHz	1 MHz triggered

Table S1. Sensor and recording details. [a] Two lasers used to make one slip velocity measurement. [b] The piezoelectric sensor output is proportional to a frequency dependent mixture of displacement and acceleration. Their output can be related to one of those quantities if the appropriate instrument response function has been removed from the raw recordings, but this has not been performed for this work. Instead, signals plotted are left in units of voltage. This voltage is the unamplified sensor output after filtering with a 7th order Butterworth 100-500 kHz bandpass filter.

DSE Name	δ_{pulse}	t_{pulse}	v_r	$\dot{\delta}_{ave}$	x_{pulse}	$\Delta\tau$	
	(μm)	(μs)	(m/s)	(mm/s)	(mm)	(Mpa)	
DSE13May2014	2.4	40	2150	60	86	0.6	1st pulse
DSE13May2014	3.2	30	2150	106.7	64.5	1.0	2nd pulse
DSE13May2014	4	50	2150	80	107.5	0.7	2nd pulse (alt. interpr.)
DSE16May2014	3.5	24	2300	145.8	55.2	1.3	last, large pulse
DSE16May2014	3.5	24	5500	145.8	132	0.5	last, large pulse (alt. interpr.)
DSE16May2014	3.8	30	5500	126.7	165	0.5	last, large pulse (alt. interpr.)
DSE16May2014	2.7	33	2200	81.8	72.6	0.7	1st pulse

Table S2. Pulse Kinematics. The data included is from four of the most prominent pulses visible in Figure 2 with alternate interpretations included to illustrate ranges of uncertainty. Time duration t_{pulse} is estimated from the slip velocity derived from the pair of laser vibrometers. Slip δ_{pulse} is derived from the time integral of the laser-vibrometer-derived slip velocity. Rupture velocity v_r is estimated from the timing of stress fluctuations detected from the array of strain gage pairs at known locations along the fault. $\dot{\delta}_{ave} = \delta_{pulse} / t_{pulse}$, $x_{pulse} = v_r \cdot t_{pulse}$, and $\Delta\tau = \mu \cdot \delta_{pulse} / x_{pulse}$, where μ is the shear modulus of the granite (20 GPa). Dynamic stress drop and maximum slip velocity may be underestimated due to the limited bandwidth of strain gages (up to 500 kHz) and laser vibrometers (up to 250 kHz). As a result, t_{pulse} and x_{pulse} reported here should be considered upper bounds. Average shear and normal stress on the fault at the onset of the DSEs were 4.8 MPa and 6.0 MPa, respectively. For comparison, total slip during DSE13May2014 was 170 μm, and total slip during DSE16May2014 was 26 μm (see Figures S2 and S3).